

# Possibilities and limitations of label-free detection of DNA hybridization with field-effect-based devices

A. Poghossian<sup>a,b,\*</sup>, A. Cherstvy<sup>c</sup>, S. Ingebrandt<sup>b</sup>, A. Offenhäusser<sup>b</sup>, M.J. Schöning<sup>a,b</sup>

<sup>a</sup> University of Applied Sciences Aachen, Division Jülich, Laboratory for Chemical Sensors and Biosensors, Ginsterweg 1, 52428 Jülich, Germany

<sup>b</sup> Institute of Thin Films and Interfaces (ISG 2), Research Centre Jülich GmbH, 52425 Jülich, Germany

<sup>c</sup> Institute of Solid-State Research, Research Centre Jülich, 52425 Jülich, Germany

Available online 30 April 2005

## Abstract

A critical evaluation of the possibilities and limitations of the label-free detection of deoxyribonucleic acid (DNA) hybridization by means of field-effect-based devices is discussed. A new DNA-detection method is introduced, which utilizes an ion-sensitive field-effect device as transducer. The upon the DNA hybridization induced redistribution of the ion concentration within the intermolecular spaces and/or the alteration of the ion sensitivity of the device is proposed as detection mechanism. The theoretical calculations predict a substantial change in the average ion concentration within the intermolecular spaces induced upon hybridization that are enough to obtain a detectable sensor signal.

© 2005 Elsevier B.V. All rights reserved.

**Keywords:** DNA; Label-free detection; Field-effect device; Ion-sensitive sensor

## 1. Introduction

Broad interest in deoxyribonucleic acid (DNA) acid microarrays or DNA chips and their growing use in genetics, medicine and drug discovery is connected with their ability to perform massive parallel sequence analysis of nucleic acids. For instance, to date about 400 diseases are diagnosable by the molecular analysis of nucleic acids, and this number is daily increasing [1]. Most of the DNA-detection techniques are based on a DNA-hybridization event. In DNA hybridization, the target (unknown single-stranded DNA (ssDNA)) is identified by a probe ssDNA and a double-stranded (dsDNA) helix structure with two complementary strands is formed. The hybridization reaction is known to be highly efficient and extremely high specific in the presence of a mixture of many different non-complementary nucleic acids. The unique complementary nature of this binding reaction between the base pairs, i.e. adenine-thymine and cytosine-guanine, is the basis for the high specificity of the biorecognition process. In general, the commonly used DNA-detection techniques

(radiochemical, enzymatic, fluorescent) are based on the detection of various labels or reagents and have been proven to be time-consuming, expensive and complex to implement. For the development of fast, simple, inexpensive and disposable genosensors, a direct label-free detection method of DNA hybridization would be favourable. In literature, different approaches for genosensors using different types of transducer principles such as cyclovoltammetric, chronopotentiometric, capacitive, impedimetric, semiconductor field effect, etc. have been described. Recent efforts in the field of genosensors and DNA chips can be found in, e.g. [1–4].

The possibility of a label-free electrical detection of the DNA-hybridization utilizing semiconductor field-effect sensors offers a new approach for a third generation of DNA chips with direct electrical readout for a fast, simple and in-expensive analysis of nucleic acid samples. The inherent miniaturization of such devices and their compatibility with advanced microfabrication technology can make them very attractive for DNA diagnostics. Therefore, in recent years, several attempts have been made to detect DNA by its intrinsic molecular charge using field-effect devices, like capacitive electrolyte-insulator-semiconductor (EIS) and field-effect transistor (FET) structures [5–16]. A DNA-FET

\* Corresponding author. Tel.: +49 2461 612605.

E-mail address: [a.poghossian@fz-juelich.de](mailto:a.poghossian@fz-juelich.de) (A. Poghossian).

is obtained by immobilizing well-defined sequences of ssDNA onto a field-effect transducer, which could convert the specific recognition process between the two complementary DNA single strands into a measurable signal. In most cases, the experimentally observed sensor response is interpreted as a result of a shift of the flat-band or threshold voltage of the field-effect structure, which arises from the binding or hybridization of the immobilized ssDNA with its complementary strand. There are, however, still insufficient experimental results and correct theoretical models for such DNA-modified field-effect devices that clearly explain their functioning principle, detection mechanism and source of the experimentally observed signal generation.

In this work, we will discuss the possibilities and limitations of a label-free detection of DNA hybridization with field-effect-based devices. A new DNA-detection method using ion-sensitive field-effect devices will be presented. The proposed method is based on the detection of the upon the DNA hybridization induced redistribution of the ion concentration within the DNA intermolecular spaces and/or the alteration of the ion sensitivity of the field-effect device.

## 2. A critical evaluation of the direct detection of DNA by its intrinsic molecular charge using field-effect devices

Field-effect devices for DNA detection reported in literature [5–16] use different sensor configurations (capacitive EIS and ES (electrolyte-silicon) structures, depletion- and enhancement-mode FET, floating-gate FET, FET devices with or without a reference electrode), different gate-insulator materials ( $\text{SiO}_2$ , silanized  $\text{SiO}_2$ ,  $\text{SiO}_2\text{-Si}_3\text{N}_4$ ,  $\text{SiO}_2\text{-poly-L-lysine}$ ) with different thicknesses (from 2 to 100 nm), various ssDNA immobilization methods (adsorption, covalent attachment, biotin–vidin complexation, linker molecules, etc.) and thus, various densities of the immobilized ssDNA from  $2.4 \times 10^8$  to  $5 \times 10^{13}$  molecules/cm<sup>2</sup>, and lastly, hybridization buffer solutions with different electrolyte concentrations (from 10  $\mu\text{M}$  to 1 M). Furthermore, the reported values of the sensor signal (mostly the flat-band or threshold voltage shift) induced upon the DNA-hybridization event reach from several mV up to  $\sim 1.9$  V and the hybridization times were between several seconds up to several hours. These results are summarized in Table 1. Due to the very large diversity of the sensor configurations and the reported results as well as due to the absence of a correct theory explaining the working principle of these devices, their comparison is very difficult. In addition, some experimentally observed effects can also not be explained in detail. For instance, it is not understandable, why a much higher signal has been observed for a sensor with a less density of the immobilized ssDNA (1.45 V with  $3.8 \times 10^8$  molecules/cm<sup>2</sup> [11]) compared to a sensor with a densely packed ssDNA (3 mV with  $5 \times 10^{13}$  molecules/cm<sup>2</sup> [7]). What is the reason for the much higher signals, which are observed when floating-gate transistors [8,10–12] or devices without a reference electrode [10,11,14] are used?

What is the working principle of DNA–FETs without a reference electrode as it was reported in [10,11,14], etc.?

In spite of the above described variety of DNA-sensor designs and reported results, they all have some principal limitations in common, which are mainly associated with the functional principle proposed for these sensors. It was suggested that in the binding event of the charged macromolecules, in particular, in the event of hybridization of the immobilized ssDNA with its complementary target molecule, the charge associated with the target molecule effectively changes the charge applied to the gate. This could measurably alter the operating characteristics of the field-effect device, e.g. the capacitance or flat-band voltage of the EIS sensor as well as the threshold voltage or the drain current of the FET-based device. In this way, a unique possibility of a direct label-free detection of DNA hybridization by means of FET devices could be given. However, it seems that due to the so-called counter-ion screening effect, a practical realization of these devices for a direct label-free detection of DNA by its intrinsic charge can yield the same well-known problems as in the case of the immuno-modified FET (see, e.g. [17,18]). It has been intensively debated, whether it would be possible to detect an antibody–antigen affinity binding reaction with an ISFET, or not [17,18]. As a result of these discussions, nowadays, it is generally accepted that the screening of protein charges by small inorganic counter ions present in the electrolyte solution will result in macroscopically uncharged layers and prevent successful measurements of immunospecies with field-effect devices. Under ideal conditions (a truly capacitive interface at which the immunological binding sites can be immobilized, a nearly complete antibody coverage, highly charged antigens and a very low ionic strength), the theoretically expected signal should be in the order of 10 mV or less [18].

Therefore, the following questions arise:

- Is it generally possible to detect a DNA-hybridization by the intrinsic charge of DNA using field-effect devices?
- How large will be a measurable signal?

Fig. 1 shows the scheme of a DNA sensor based on a capacitive EIS (a) and FET (b) structure, respectively. Generally, there are a number of ways in which the DNA hybridization can affect the electrical properties of the interface. In the case of field-effect devices, two basic effects are usually considered: (i) a geometrical capacitance effect (due to the displacement of electrolyte by the target molecules and change in the “effective” thickness of the gate insulator and thus, change in the “effective” gate capacitance) and (ii) a charge effect. Dependent on the type of doped semiconductor substrate, these two effects can affect the sensor signal in the same direction, or in opposite direction and thus, to some extent, they might even compensate each other. This could be used to determine which effect, either the capacitance or the charge effect is dominating the sensor output. In this work, we will focus on the charge effect.

Table 1  
Summary of field-effect-based DNA sensors discussed in literature

| Sensor type  | Probe DNA; immobilization; density  | Electrolyte; buffer                     | Target DNA   | Sensor signal   | Hybridization time | RE                      | Reference |
|--|---|---|--|---|--------------------|-------------------------|-----------|
| EIS; FET <i>p</i> -Si-SiO <sub>2</sub> (10 nm, silanization with APTES)  | Oligo(dT <sub>20</sub> ); poly(dT) (1000 bases); brominated oligonucleotides        | 50 mM NaCl; 10 mM Tris-HCl, pH 7.1      | Oligo(dA <sub>18</sub> ); poly(dA) (1000 bases); calf thymus DNA | $\Delta V_{FB} \sim 100$ mV; $\Delta V_{Th} \sim 120$ mV at 2 $\mu$ g/ml target DNA                         | 4 h                | Ag/AgCl                 | [5]       |
| EIS; <i>p</i> -Si-SiO <sub>2</sub> (30 nm)-Si <sub>3</sub> N <sub>4</sub> (26 nm)  | Oligo(dC <sub>30</sub> ); covalent or adsorption; coverage: <3%                     | 2 $\times$ saline sodium citrate buffer | Oligo(dG <sub>30</sub> )   | Normal device: insensitive; scratched device: $\Delta C \sim 2.7$ –3.2%                                     | Several seconds    | Pt                      | [15]      |
| <i>p</i> -Si   | 10-Mer ssDNA; covalent  | 0.5 M MgCl <sub>2</sub> , pH 8          | 10-Mer ssDNA   | $\Delta C \sim 0.2\%$ $\Delta V_{Th} \sim 0.3$ –0.4 V   | 10–20 s            | Calomel electrode       | [9]       |
| <i>n</i> -Si-SiO <sub>2</sub> (2 nm)-poly-L-lysine   | 12-Mer ssDNA; adsorption  | 23 mM                                   | 12-Mer ssDNA   | $\Delta V_{FB} \sim 3$ mV; differential response  | 10–15 min          | Ag/AgCl                 | [7]       |
| Au-gate <i>n</i> -channel depletion FET; <i>p</i> -Si-SiO <sub>2</sub> (63 nm)-Si <sub>3</sub> N <sub>4</sub> (30 nm)-Au | Thiolated 15- or 25-mer ssDNA   | 1 M NaCl; pH 7.4                        | 15-Mer ssDNA<br>25-Mer ssDNA                                     | $\Delta k \sim 3\%$ ; $\Delta V_{Th} \sim 10$ mV<br>$\Delta I_d \sim 0.4$ $\mu$ A $\Delta V_{Th} \sim 3$ mV | 1000 s             | Ag wire                 | [8]       |
| <i>n</i> -channel FET; <i>p</i> -Si-SiO <sub>2</sub> -Si <sub>3</sub> N <sub>4</sub> ; silanization with APTES           | 26-Mer ssDNA; avidin-biotin complexation  | Not reported                            | 26-Mer ssDNA   | Sensitivity: 456 mV/ $\mu$ g/ $\mu$ l   | 2 h                | Calomel electrode       | [6]       |
| <i>n</i> -channel FET; <i>p</i> -Si-SiO <sub>2</sub> (50 nm)   | 20-mer ssDNA; adsorption  | Phosphate buffer, pH 7                  | Detection of probe ssDNA   | $\Delta I_d \sim 20$ $\mu$ A or $\Delta V_{Th} \sim 1.9$ V  | 3.5 h              | Without RE              | [14]      |
| <i>p</i> -channel FET; <i>n</i> -Si-SiO <sub>2</sub> (8–12 nm); silanization with APTES                                  | Adsorption<br>$\sim 4 \times 10^{11}$ molecules/cm <sup>2</sup>                     | 1 mM NaCl                               | PolyA, 20 or 45 bases  | $\Delta V_{Th} \sim 5$ mV   | $\sim 1$ h         | Ag/AgCl liquid-junction | [13]      |
| <i>p</i> -channel Au-gate (floating) FET; <i>n</i> -Si-SiO <sub>2</sub> (50 nm)  | 12-Mer thiol-modified ssDNA, spacer;<br>$3.5 \times 10^8$ molecules/cm <sup>2</sup> |   | 12-Mer ssDNA   | $\Delta V_{Th} \sim 0.87$ V   | Several minutes    | Without RE              | [10]      |
| <i>p</i> -channel Au-gate (floating) FET; <i>n</i> -Si-SiO <sub>2</sub> (50 nm)  | 15-Mer thiol-modified ssDNA, spacer;<br>$2.4 \times 10^8$ molecules/cm <sup>2</sup> | Phosphate buffer saline, pH 7.4         | 15-Mer ssDNA   | $\Delta V_{Th} \sim 0.23$ V   |                    | Pt                      | [12]      |
| <i>p</i> -channel Au-gate (floating) FET; <i>n</i> -Si-SiO <sub>2</sub> (50 nm)  | 15-Mer thiol-modified ssDNA, spacer;<br>$3.8 \times 10^8$ molecules/cm <sup>2</sup> | Phosphate buffer                        | 15-Mer ssDNA   | $\Delta V_{Th} \sim 1.45$ V by immobilization,<br>$\Delta I_d \sim 10$ –15 $\mu$ A by hybridization         |                    | Without RE              | [11]      |
| <i>p</i> -channel FET; <i>n</i> -Si-SiO <sub>2</sub> (10 nm)-poly-L-lysine   | 20-Mer dsDNA;<br>$2 \times 10^{13}$ molecules/cm <sup>2</sup>                       | 0.01 mM KCl<br>1 mM<br>>10 mM           | Detection of dsDNA   | 80 mV<br>40 mV<br><10 mV  |                    | Ag/AgCl wire            | [16]      |

$\Delta V_{FB}$ : flatband-voltage change;  $\Delta V_{Th}$ : threshold-voltage change;  $\Delta I_d$ : drain-current change;  $\Delta k$ : transconductance change; RE: reference electrode; APTES: 3-aminopropyltriethoxysilane.

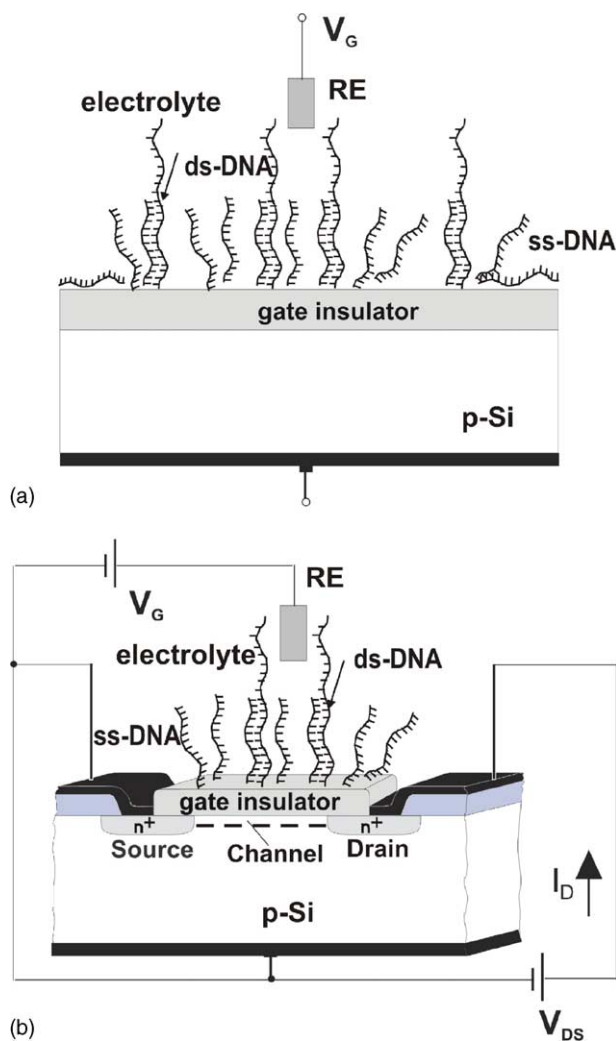


Fig. 1. Scheme of the DNA sensor based on a capacitive EIS (a) and FET (b) structure. RE: reference electrode;  $V_G$ : gate voltage;  $V_{DS}$ : source-drain voltage;  $I_D$ : drain current.

Field-effect devices are basically surface-charge measuring devices (they detect the charge in a capacitive way) and therefore, they can principally measure the charge of adsorbed macromolecules or the charge change due to a hybridization event. For operating, a voltage is applied via a reference electrode, which is also responsible for fixing the potential of the analyte solution. The electric field in the gate insulator depends on, among other parameters, the net surface charge at the electrolyte-insulator interface. Any charge changes at the insulator surface will result in an equal change in the charge density of opposite sign in the semiconductor space-charge region. Since DNA molecules are poly-anions with negative charges at their phosphate backbone, it could be expected that the hybridization of ssDNA with its complementary strands would directly modulate the capacitance of the EIS structure or the drain current of the FET device. However, this scheme for the detection of charged macromolecules is only feasible, if the charges cannot cross the interface (i.e. the interface is ideally polarized), which

thus behaves as a perfect capacitor. In reality, no interface is ideally polarized and must be modeled as a capacitor in parallel with a charge transfer resistor. Therefore, the principal practice problem with a molecular charge measurement is to transduce the molecular recognition action between the probe ssDNA and the target molecule into a measurable signal. It is obvious that the charge distribution in the immediate vicinity of the interface plays a critical role in transferring the upon hybridization induced signal to the field-effect transducer.

### 2.1. How large can be the charge change induced upon DNA hybridization?

Only charge-density changes, which occur on the surface or within the order of the Debye length,  $\lambda_D$ , from the surface can be detected:

$$\lambda_D = \left( \frac{\varepsilon_{el}\varepsilon_0 kT}{2z^2 q^2 I} \right)^{1/2} \quad (1)$$

where  $k$  is the Boltzmann constant,  $T$  the absolute temperature,  $\varepsilon_0$  the permittivity of vacuum,  $\varepsilon_{el}$  the dielectric constant of the electrolyte,  $z$  is the valency of the ions in the electrolyte,  $q$  is the elementary charge and  $I$  represents the ionic strength, which for a 1–1 salt, can be replaced by the electrolyte concentration,  $n_0$ .

Fig. 2 schematically illustrates this situation. Here, exemplarily a 10-bases DNA molecule is shown normal to the surface of the field-effect sensor. As can be seen, with increasing ionic strength of the electrolyte, the fraction of DNA charge, which remains in the double layer and thus, will be mirrored in the sensor (e.g. in the channel of the transistor structure), is decreased. For instance, in physiological solutions with  $\lambda_D \approx 0.8$  nm, most of the DNA charge will be at a distance greater than the Debye length from the surface. Moreover, the DNA charge is not confined directly to the interface, but it is distributed through some distance (dependent on the number of base pairs) away from the surface. Thus, the fraction of charge mirrored in the inversion layer will be even smaller. If ssDNA molecules are immobilized using linker molecules or spacers, the upon DNA hybridization induced charge changes will be still smaller. On the other hand, if DNA molecules preferentially lie flat on the surface, a higher hybridization signal can be expected [19].

In addition, the charge associated with the probe- or target-DNA molecules can be screened or neutralized (in whole or part) by small counter ions present in the solution (Fig. 3). According to Manning's counter-ion condensation theory [20,21], monovalent cations reduce the DNA charge by 76% and divalent cations by 88%. The remaining charge will be compensated by the more diffuse ionic layer, where the charge density decreases exponentially with distance from the DNA surface [22]. According to [23], the full release of counter ions condensed onto a highly charged rod (such as DNA) is not always observed in the vicinity of an even oppositely charged surface. This counter-ion condensation effect

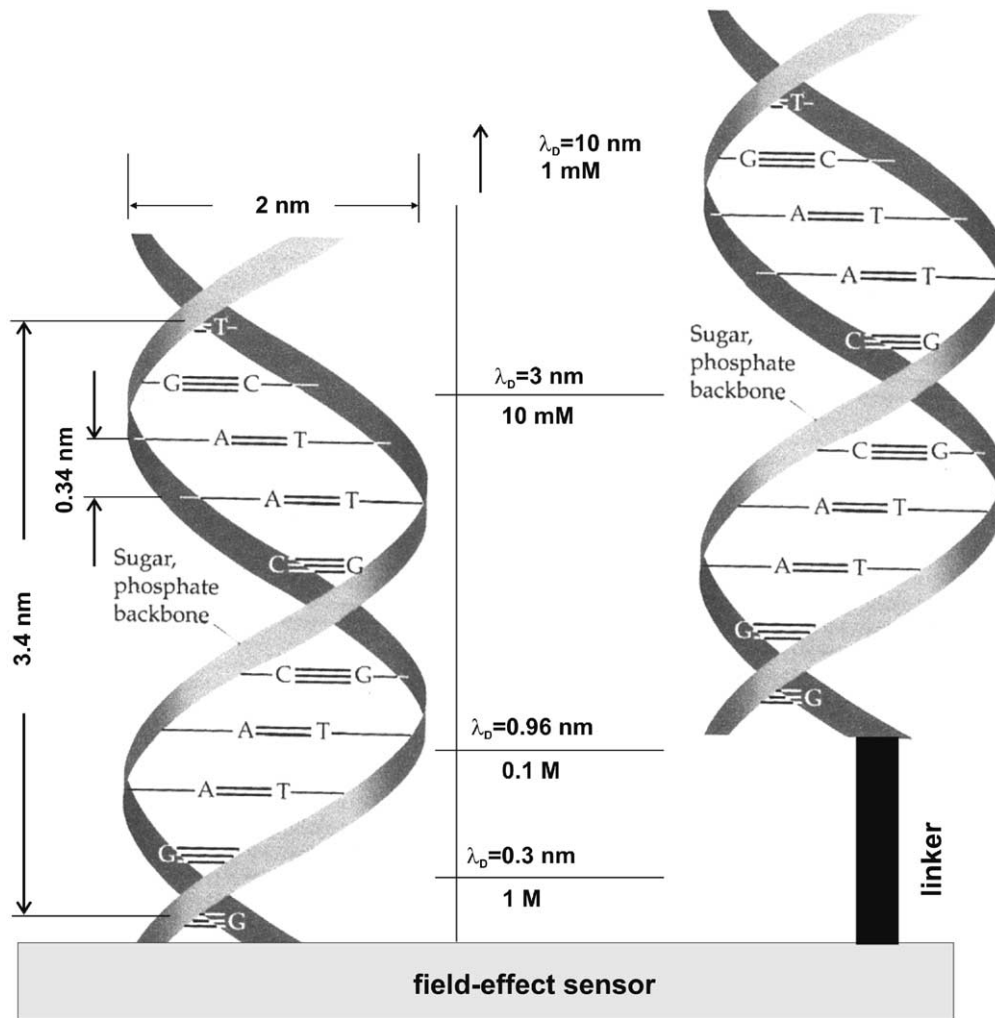


Fig. 2. Schematic illustration of a 10-bases DNA molecule oriented normal to the sensor surface and Debye length,  $\lambda_D$ , in electrolyte with different ionic strengths. With increasing ionic strength of the electrolyte solution, the fraction of DNA charge that remains in the double layer and thus, will be mirrored in the field-effect sensor, is decreased.

will mask or reduce the expected hybridization signal and prevent successful measurements, especially in high ionic-strength solutions. Thus, although a charged target molecule has bound to the immobilized probe molecule, the hybridized

pair produces a net reduced or even zero charge. As a result, at the interface between the dsDNA layer and sensor surface, the electric field can be insignificant or nearly zero and thus, the underlying field-effect transducer is practically not influenced and no sensor signal can be observed.

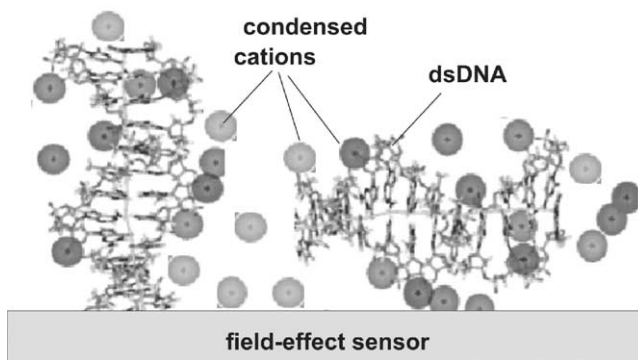


Fig. 3. Compensation of the DNA charge by condensed counter ions (schematically).

Let us estimate the FET-sensor signal (i.e. the change in the electrolyte/gate insulator interface potential) induced upon the DNA-hybridization process. It is still very little known about the composition of the DNA/sensor interface, which plays a critical role in the signal generation. Nevertheless, in a first approach, the hybridization of the probe molecules with their complementary target molecules can be modeled as a transfer of a certain quantity of the charge,  $Q_h$ , from the solution to the surface of the gate insulator. Since electroneutrality must be observed in the system, an equal quantity of the opposite charge must be either enter in the inversion layer of the FET or enter the double layer from the solution. The charge change,  $Q_i$ , on the capacitance of the gate insulator,  $C_i$ , which is mirrored in the inversion layer of the FET, can

be represented by [18]:

$$Q_i = \frac{Q_h C_i}{C_i + C_{dl}} \quad (2)$$

where  $C_{dl}$  is the capacitance of the double layer. The estimations using typical values for  $C_{dl} = 20 \mu\text{F}/\text{cm}^2$  [24] and  $C_i = 0.35 \mu\text{F}/\text{cm}^2$  for 10 nm thick  $\text{SiO}_2$ , give  $Q_i/Q_h \sim 0.017$ . Thus, only about 1.7% of the upon hybridization induced charge will be mirrored in the transistor. The remaining charge will be compensated by the ions in the solution. The charge change that is induced upon hybridization can be described as:

$$Q_h = mN\alpha(1 - \theta) \quad (3)$$

where  $m = q\lambda_D/b$  is the fraction of DNA charge in the double layer (for simplicity, DNA molecules are considered arranged normal to the surface and with one negative charge per base pair),  $b$  is the distance between the nearest unit charges along the DNA,  $N$  is the density of the immobilized probe molecules,  $\alpha$  is the hybridization efficiency and  $\theta$  is the fraction of DNA charge compensated by the condensed cations. With this, the interfacial potential change due to the hybridization (i.e. the expected sensor signal) can be defined as:

$$\varphi = \frac{Q_i}{C_i} = mN\alpha \frac{1 - \theta}{C_i + C_{dl}} \quad (4)$$

The calculations using expression (4) and typical values of  $C_{dl} = 20 \mu\text{F}/\text{cm}^2$ ,  $C_i = 0.35 \mu\text{F}/\text{cm}^2$ ,  $\lambda_D = 1 \text{ nm}$  (for a 0.1 M electrolyte solution),  $N = 10^{12}$  molecules/ $\text{cm}^2$ ,  $b = 0.34 \text{ nm}$  and  $\theta = 0.76$  show that the hybridization signal will be just several mV of amplitude ( $\varphi = \sim 3 \text{ mV}$  with a hybridization efficiency of 50% ( $\alpha = 0.5$ ) and  $\varphi = \sim 6 \text{ mV}$  with a 100% hybridization efficiency ( $\alpha = 1$ )).

To reduce the counter-ion screening effect and thus, to enhance the sensitivity of the sensor, such devices must be operated in very low ionic-strength solutions. The price to be paid is a reduced probability of hybridization (due to the electrostatic repulsion between the complementary DNA strands) and therefore, an extended hybridization time and reduced signal. According to estimations performed in [7,13] using the Graham equation, the expected hybridization signal could be in the mV range ( $\sim 3 \text{ mV}$  from the  $3 \times 10^{12}$  hybridized 12-mer DNA/ $\text{cm}^2$  in an electrolyte solution with an ionic strength of 23 mM [7], and  $\sim 0.8 \text{ mV}$  from the  $4 \times 10^{11}$  hybridized 20-mer DNA/ $\text{cm}^2$  in a solution with an ionic strength of 1 mM [13]).

A further problem is, that for a correct functioning of the field-effect devices for DNA detection by its intrinsic charge, the surface interaction should only occur between the immobilized ssDNA and its complementary target. The signal should not be interfered by any background interaction of the underlying gate surface with ions presented in the solution. Therefore, in order to “insulate” the underlying gate from the solution, the immobilized probe molecules should form a perfectly homogeneous and tightly packed

monolayer without any pores or interstitial spaces. However, the theoretical jamming coverage, i.e. the maximum surface coverage, has been calculated to be  $\sim 25\text{--}35\%$  for a random-sequential adsorption of rod-like molecules [25]. Many experimental results also show that the adsorbed layers of macromolecules are much less dense (see, e.g. [13,14]), which can allow an interstitial penetration of small inorganic ions and water molecules to the underlying gate layer that can be, for example, pH-, ion- or redox-sensitive. In addition, changes in the interstitial water and ion distribution induced during the hybridization event can significantly screen the charge effect of the DNA molecules, thereby reducing the overall magnitude of the field-effect [26].

Thus, all of the above discussed effects as well as the possible adsorption of macromolecules onto the reference- or pseudo-reference electrode, sensor drift and leakage current can result in masking, reducing or interfering with the upon hybridization induced signal of interest, and even may result in a false signal interpretation. In this context, the reported experiments with the floating-gate transistors [8,10–12] or with the pseudo-reference electrodes such as Ag or Pt wires [8,12,15,16] should be carefully evaluated, and measurements without a reference electrode [10,11,14] should be considered as very questionable. To perform correct measurements, other parameters, like pH, ionic strength, temperature and potential of the reference electrode must be constant. It is always favorable to use differential measuring set-ups to exclude some of these disturbing or interfering effects.

Generally, it could be concluded that a practical realization of field-effect devices for the pure electrostatic detection of charges associated with the probe or target molecules in relatively high ionic-strength solutions (e.g. in physiological solutions) is problematic. The expected hybridization signals could be in the range of several mV. Therefore, the theoretical basis of the sometimes experimentally observed results, in particular, the large sensor signals, still remains unclear. Therefore, much more theoretical (modeling) and experimental research has to be done in order to understand and correctly interpret the DNA-hybridization detection experiments with field-effect devices.

### 3. A new method for the label-free detection of DNA hybridization by means of ion-sensitive field-effect devices

As an alternative, we propose a new method for the label-free DNA detection using an ion-sensitive field-effect device (or device that senses the changes in the ionic strength of the electrolyte), whose top surface is modified with immobilized ssDNA probe molecules arranged with a center-to-center average interprobe distance  $a_s$  (Fig. 4). The interprobe distance  $a_s$  should be considered as a statistically averaged distance. The remaining surface of the ion-sensitive layer between the immobilized molecules is in contact with

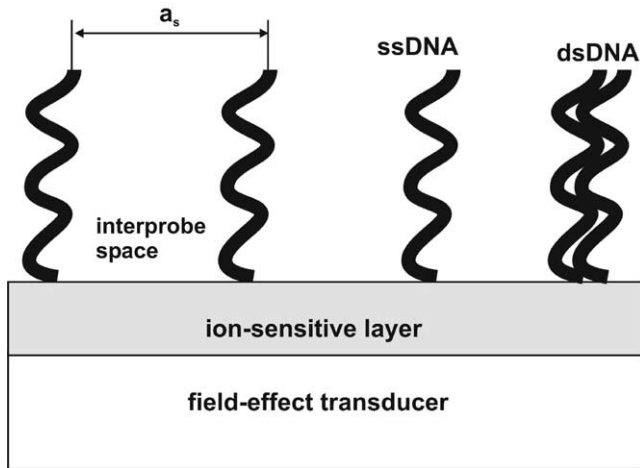


Fig. 4. DNA sensor based on an ion-sensitive field-effect device (schematically). The immobilized ssDNA probe molecules are arranged onto the ion-sensitive layer with a center-to-center average interprobe distance  $a_s$ .

the electrolyte solution. In this work, the term “ion-sensitive layer” is related not only to different conventional and non-conventional ion-sensitive materials, but also to the materials that are sensitive to a change in the ionic strength of the electrolyte or mixed potentials.

Generally, such a model corresponds to the real situation, since in most experiments usually the immobilized ssDNA (as well as dsDNA) molecules do not form perfectly homogeneous and tightly packed monolayers. Moreover, the probe ssDNA molecules should be arranged on the surface with enough interstitial space to allow a rapid hybridization and to provide a high hybridization efficiency. A preferable average center-to-center separation distance could be in the range from  $\sim 2.5$  to  $\sim 10$  nm that corresponds to a probe density from about  $2 \times 10^{13}$  to  $1.3 \times 10^{12}$  molecules/cm<sup>2</sup>, typically reported in the literature [2,27–29].

In Fig. 4, for simplicity, the ssDNA is presented as rod-like molecule oriented normal to the sensor surface. In a more realistic picture, the ssDNA is a flexible coil-like molecule. Dependent on the immobilization method, length of ssDNA and the surface conditions, ssDNA molecules can lie flat on the sensor surface with the phosphate groups or bases exposed to the surrounding solution; they can be oriented normal or with a certain angle to the surface as well as can have one or several contacts with the sensor surface. After hybridization, short fragments of the dsDNA will remind rather rod-like than coil-like, as known.

Our proposed device detects the hybridization of the probe molecule with its complementary strand by sensing:

- (1) the redistribution of the ion concentration in the intermolecular spaces induced upon the hybridization and/or
- (2) the alteration of the ion sensitivity of the transducer caused by the hybridization.

Resulting changes in the potential at the interface ion-sensitive layer/electrolyte within intermolecular regions,

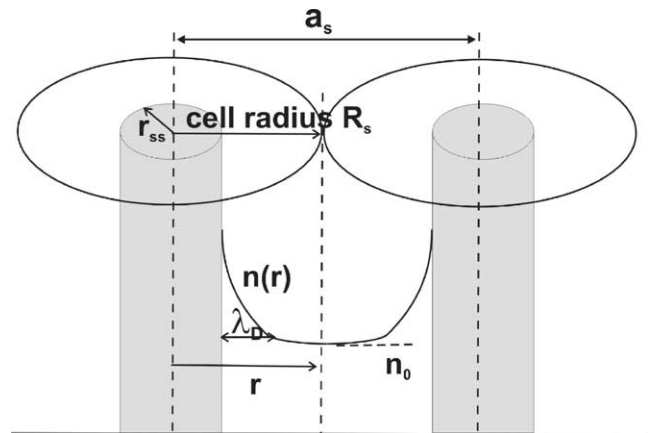


Fig. 5. Cell model for the theoretical description of the ion-concentration redistribution in the intermolecular spaces upon DNA hybridization. The ssDNA and dsDNA (not shown) form a hexagonal lattice of uniformly negatively charged, infinitely long cylinders with a radius  $r_{ss} = 5 \text{ \AA}$  and  $r_{ds} = 10 \text{ \AA}$ , respectively. The cylinders are arranged normal to the sensor surface with a center-to-center average separation distance of  $a_s \approx 2R_s$ .  $R_s$ : DNA-cell radius;  $n(r)$ : ion concentration as a function of the coordinate  $r$  from the DNA axis;  $n_0$ : bulk ion concentration.

which are induced by the hybridization process, can be detected by the ion-sensitive field-effect sensor.

### 3.1. Ion-concentration redistribution in the intermolecular spaces upon the DNA hybridization

The theoretical model for the proposed device concept is presented in Fig. 5. It is suggested, that the ssDNA or dsDNA molecules form a hexagonal lattice with a cell radius of  $R_s$ , modeled below as the lattice of uniformly negatively charged, infinitely long cylinders with a radius  $r_{ss} = 5 \text{ \AA}$  and  $r_{ds} = 10 \text{ \AA}$ , respectively. The cell model has been successfully used for the description of DNA–DNA electrostatic interaction in dense assemblies [30]. The cylinders are oriented normal to the sensor surface with a center-to-center average separation distance of  $a_s = R_s \sqrt{2\pi/\sqrt{3}} \approx 2R_s$ . The effect of DNA hybridization is modeled by doubling of the linear charge density of the cylinder and by increasing the cylinder radius from 5 to 10  $\text{\AA}$ .

Because in a broad pH range (from pH 4 to 11) ssDNA and dsDNA molecules are negatively charged via their phosphate groups, such negatively charged molecules will attract positively charged counter ions (including protons) from the solution and repel the co-ions. In equilibrium, a certain distribution of the electrostatic potential emerges around the DNA molecules. The characteristic length of the potential decay is the Debye screening length,  $\lambda_D$ , which determines the thickness of the double layer formed by the ions around the DNA. As a result, the DNA charge is effectively compensated by the surrounding small counter ions. This may result in a local ion-concentration redistribution within the intermolecular spaces (increasing the cation concentration and decreasing the anion concentration) that can substantially

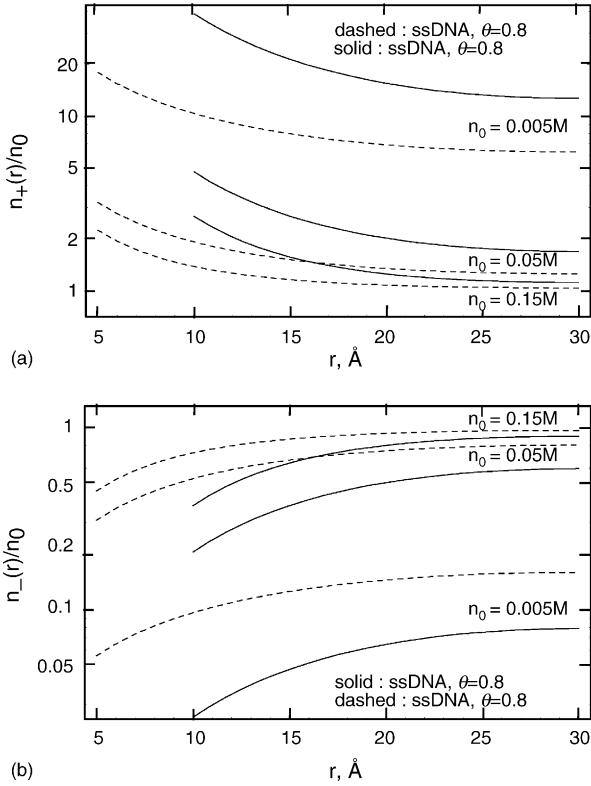


Fig. 6. Calculated distribution of the cations ( $n_+(r)/n_0$ ) (a) and anions ( $n_-(r)/n_0$ ) (b) in the intermolecular spaces before (dotted curves) and after hybridization (solid curves) as a function of the coordinate  $r$  from the DNA axis for  $R_s = 3$  nm,  $\theta = 0.8$  and in a 1:1 electrolyte with different bulk concentrations of 0.005, 0.05, and 0.15 M, respectively.

differ from the concentration in the bulk electrolyte,  $n_0$ . After hybridization, because the charge of the dsDNA is nearly doubled, a new distribution of the electrostatic potential and of the ions within the intermolecular spaces will be reached.

Fig. 6 shows the calculated distribution of the cations ( $n_+(r)/n_0$ ) and anions ( $n_-(r)/n_0$ ) in the intermolecular spaces before (dotted curves) and after hybridization (solid curves) as a function of the coordinate  $r$  from the DNA axis for  $R_s = 3$  nm,  $\theta = 0.8$  and in a 1:1 electrolyte with different bulk concentrations of 0.005, 0.05, and 0.15 M, respectively. The calculations have been made using the equations for the electrostatic potential derived in [31], where a linearization of the Poisson–Boltzmann equation near the Donnan potential in the hexagonal DNA cell was implemented. As it can be seen, the local counter- and co-ion concentration within the intermolecular spaces substantially differ from that of the bulk solution. Moreover, the ion-concentration distribution after the hybridization differs substantially from the situation before hybridization (i.e. in the presence of the immobilized ssDNA only). Thus, in contrast to the above discussed field-effect devices for the DNA-hybridization detection by the intrinsic molecular charge, here, namely the counter-ion condensation effect is used to detect the DNA-hybridization event.

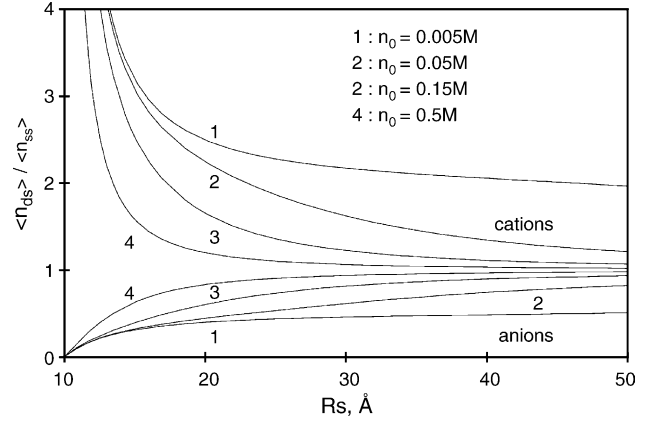


Fig. 7. Ratio  $\langle n_{ds} \rangle / \langle n_{ss} \rangle$  of average concentration of cations and anions within the intermolecular spaces after hybridization ( $\langle n_{ds} \rangle$ ) and before hybridization ( $\langle n_{ss} \rangle$ ) as function of the DNA-cell radius  $R_s$  and in 1:1 salt solutions with bulk ion-concentration of  $n_0 = 0.005, 0.05, 0.15$ , and  $0.5$  M, respectively.

For sensor applications, a more interesting parameter is the degree of change in the average ion concentration in the intermolecular spaces upon hybridization. Following the procedure described in [32], the average concentration of cations and anions in the intermolecular spaces can be presented as:

$$\langle n_{\pm}(R_s) \rangle = n_0(\pm\zeta + \sqrt{\zeta^2 + 1}) \quad (5)$$

where

$$\zeta = \frac{1 - \theta}{2\pi b n_0 (R_s^2 - a^2)} \quad (6)$$

$b$  is the distance between the nearest unit charges along the cylinder ( $b = 0.34$  nm for the ssDNA and  $b = 0.17$  nm for the dsDNA) (+) and (–) are related to cations and anions, respectively, and  $a = r_{ss}$  for the ssDNA and  $a = r_{ds}$  for the dsDNA.

As an example, Fig. 7 shows the ratio  $\langle n_{ds} \rangle / \langle n_{ss} \rangle$  of the average concentration for cations and anions within the intermolecular spaces after hybridization ( $\langle n_{ds} \rangle$ ) and before hybridization ( $\langle n_{ss} \rangle$ ) as a function of the DNA-cell radius  $R_s$  and in 1:1 salt solutions of different bulk ion concentrations of  $n_0 = 0.005, 0.05, 0.15$  (physiological solution), and  $0.5$  M, respectively. The fraction of both ssDNA and dsDNA charge compensated by the condensed cations was taken as  $\theta = 0.7$ , which is a good approximation for a 1:1 salt solution.

As it can be seen from Fig. 7, the average ion concentration within the intermolecular spaces after the hybridization clearly differs from that of before the hybridization event. The difference would be enough to obtain a detectable sensor signal even in high ionic-strength solutions (0.5 M), where the hybridization efficiency is high and the hybridization event can be faster. For instance, by assuming a high density of the immobilized ssDNA of about  $2 \times 10^{13}$  molecules/cm<sup>2</sup> ( $a_s = 2R_s \sim 25$  Å) and under the assumption of a 100% hybridization efficiency, the average ion concentration within the intermolecular spaces after hybridization can be more than three to four times higher (for cations) and less (for

anions) than that before the hybridization event. If, for example, the ion-sensitive field-effect device possesses a typical Nernstian slope, such a change in the ion concentration, induced upon hybridization would correspond to a change in the sensor signal of about 28–35 mV. The effect is dependent on the ionic strength of the bulk electrolyte solution and stronger in a low ionic-strength electrolyte. Such a dependence of the signal amplitudes on the ion concentration has been observed in DNA immobilization and hybridization experiments with a FET structure, e.g. in [13]. By decreasing the density of the immobilized ssDNA molecules (i.e. with increasing  $R_s$ ), the ratio  $\langle n_{ds} \rangle / \langle n_{ss} \rangle$  is decreased, more strongly in high ionic-strength solutions. Therefore, to obtain a high hybridization signal at a low density of the immobilized ssDNA, measurements in low ionic-strength solutions could be favorable. The ratio  $\langle n_{ds} \rangle / \langle n_{ss} \rangle$  is strongly increased at a small separation distance (high density of the immobilized ssDNA). However, at the same time, the “useful” sensor area, available for the ion interaction, is decreased. Therefore, dependent on the sensor design, the optimum separation distance or optimum density of the immobilized ssDNA can be found in order to achieve a maximal hybridization signal. In principle, an increase in the hybridization signal of about two times can be achieved by using a device, which combines both a cation- and an anion-sensitive sensor in a differential measuring set-up.

Similar ion-redistribution effects induced upon hybridization could also take place when ssDNA probe molecules lie flat onto the sensor surface or are oriented with a certain angle to the surface. Furthermore, the estimations for average ion concentration in DNA lattice using a more realistic model, considering the DNA molecules as charged spirals, do not change the described effects qualitatively. In many relevant applications, the ssDNA are often attached to the surface via linker molecules. The calculation of the electrostatic potential near to the end of the DNA rod of a finite length placed at a certain distance from the surface, shows a strong dropping of the potential with increasing distance between the DNA molecule and the surface [32]. Therefore, if the ssDNA molecules are immobilized using longer linker molecules, one should not expect a high hybridization signal. In addition, it should be noted that the presented model does not take into account the charge state of the sensor surface; theoretical models, which also include an effect of the surface charge, are more complicated. Nevertheless, in a first approach it can be expected that the diffuse layer of counter ions around the DNA will overlap with the diffuse layer of the electrolyte/ion-sensitive layer interface. As a consequence, a three-dimensional redistribution of the ion concentration in the intermolecular spaces upon hybridization can be predicted.

### 3.2. Alteration of the ion sensitivity of the ion-sensitive layer upon the hybridization

In addition to the ion-concentration redistribution effect in the intermolecular spaces, upon the hybridization the ion sensitivity of the ion-sensitive layer can be modulated. For

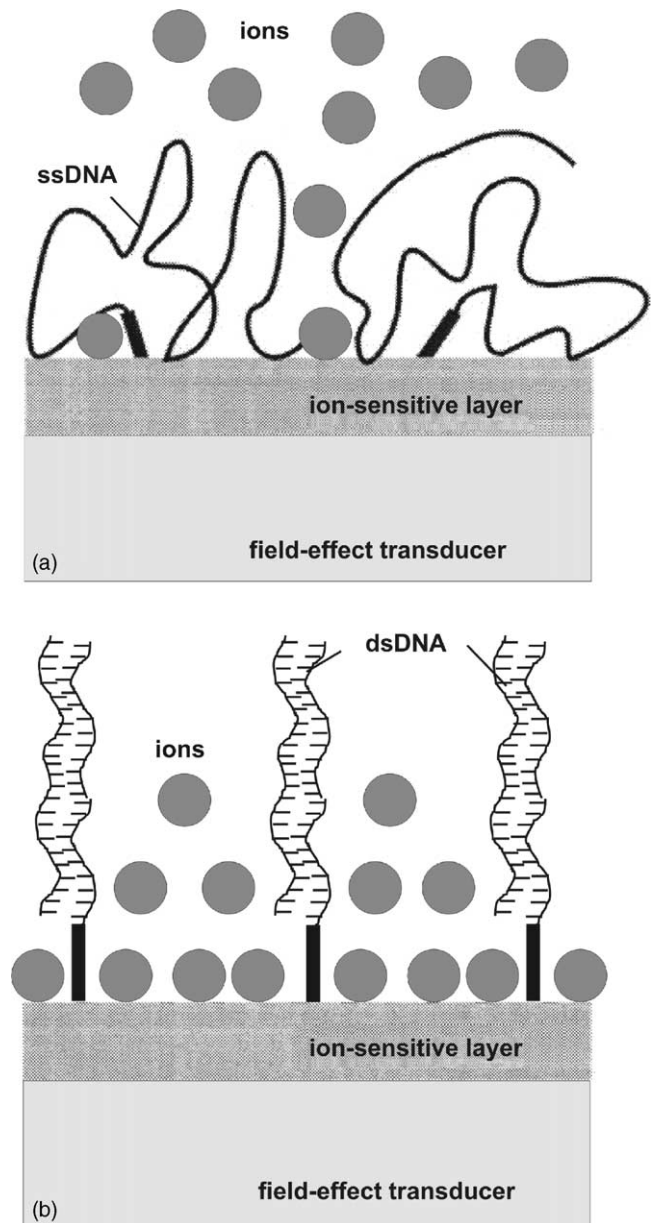


Fig. 8. Alteration of the ion sensitivity of the ion-sensitive layer as a possible mechanism for DNA hybridization detection with a field-effect device (schematically). The flexible ssDNA molecules can cover, screen and thus, alter the effective amount of the surface sites available for an ion interaction, or they can prevent potential-determining ions from reaching the ion-sensitive surface (a). After hybridization, a rigid rod-like dsDNA is formed, thus opening the surface of the ion-sensitive layer to ions (b).

instance, if the flexible ssDNA molecules lie preferentially flat on the ion-sensitive layer, they can cover, screen and thus, alter the effective amount of surface sites of the ion-sensitive layer available for an interaction (e.g. ion-binding or ion-exchange processes) with the ions in the solution or they can prevent potential-determining ions from reaching the ion-sensitive surface (Fig. 8(a)). In contrast, after hybridization a rigid rod-like dsDNA is formed, thus opening the surface of the ion-sensitive layer to ions (Fig. 8(b)), which can result

in an additional change of the sensor signal. According to these very elementary considerations of disturbances in the ion-diffusion and/or ion-binding (ion-exchange) processes, we can predict an alteration of the ion sensitivity of the ion-sensitive layer, which can result in an additional change of the sensor signal.

#### 4. Conclusions

Generally, it can be concluded that the practical development of field-effect devices for the direct label-free detection of DNA hybridization by its intrinsic molecular charge appears to be more difficult than expected. The theoretical basis of the sometimes observed results and especially, the wide variety of the reported signal amplitudes and response times, still remains unclear. Therefore, the reported experimental results, concerning the DNA detection by means of field-effect devices, should carefully be evaluated. Moreover, a correct functioning of these devices without a reference electrode in the electrolyte solution should be discussed as very questionable.

A new label-free DNA-detection method and device strategy utilizing an ion-sensitive field-effect sensor is introduced and discussed. In contrast to field-effect-based DNA sensors of the prior art discussed in Section 2, we suggest the use of the upon the DNA hybridization induced redistribution of the ion concentration within the intermolecular spaces and/or an alteration of the ion sensitivity as a detection mechanism. The theoretical calculations predict a substantial change in the average ion concentration within the intermolecular spaces before and after hybridization, enough to obtain a detectable sensor signal. The proposed device concept, in principle, would be capable for functioning in both low- and high ionic-strength solutions.

Nonetheless, there are still insufficient experimental results with DNA-FETs to clearly understand their functioning. This situation might be improved in the near future and much effort will be directed towards new experiments with the DNA-FETs and the development of theoretical models, which will further explain the experimental results. The discussed subject is quite complicated and interdisciplinary, and at the same time, highly important. A deep understanding of the adsorption and interaction of DNA and other charged biomolecules onto charged surfaces is of great interest not only for sensor applications, but also for the fundamental understanding of many key physiological processes. Therefore, a combination of knowledge and collaboration of scientists from bio- and electrochemistry, macromolecular physics, surface and device physics, etc. is necessary for the development of correct theoretical models and future experiments.

#### Acknowledgements

The authors thank M. Keusgen for valuable discussions. Part of this work was supported by the Ministerium für

Bildung und Forschung des Landes Nordrhein-Westfalen, Germany.

#### References

- [1] C.H. Mastrangelo, DNA analysis systems on a chip, in: P. Vincenzini, L. Dori (Eds.), *Solid-State Chemical and Biochemical Sensors*, Techna, Faenza, 1999, pp. 465–476.
- [2] M.C. Pirrung, How to make a DNA chip, *Angew. Chem. Int. Ed.* 41 (2002) 1276–1289.
- [3] M.J. Heller, DNA microarray technology: devices, systems, and applications, *Annu. Rev. Biomed. Eng.* 4 (2002) 129–153.
- [4] P. de-los-Santos-Alvarez, M. Jesus Lobo-Castanon, A.J. Miranda-Ordieres, P. Tunon-Blanco, Current strategies for electrochemical detection of DNA with solid electrodes, *Anal. Bioanal. Chem.* 378 (2004) 104–118.
- [5] E. Souteyrand, J.P. Cloarec, J.R. Martin, C. Wilson, I. Lawrence, S. Mikkelsen, M.F. Lawrence, Direct detection of the hybridization of synthetic homo-oligomer DNA sequences by field effect, *J. Phys. Chem. B* 101 (1997) 2980–2985.
- [6] G. Libo, H. Jinghong, Z. Hong, C. Xiang, DNA field-effect transistor, *Proc. SPIE* 4414 (2001) 47–49.
- [7] J. Fritz, E.B. Cooper, S. Gaudet, P.K. Sorger, S.R. Manalis, Electronic detection of DNA by its intrinsic molecular charge, *PNAS* 99 (2002) 14142–14146.
- [8] F.K. Perkins, L.M. Tender, S.J. Fertig, M.C. Peckerar, Sensing macromolecules with microelectronics, *Proc. SPIE* 4608 (2002) 251–265.
- [9] F. Wei, B. Sun, Y. Guo, X.S. Zhao, Monitoring DNA hybridization on alkyl modified silicon surface through capacitance measurement, *Biosens. Bioelectron.* 18 (2003) 1157–1163.
- [10] D.-S. Kim, Y.-T. Jeong, H.-K. Lyu, H.-J. Park, H.S. Kim, J.-K. Shin, P. Choi, J.-H. Lee, G. Lim, M. Ishida, Fabrication and characteristics of a field-effect transistor-type charge sensor for detecting deoxyribonucleic acid sequence, *Jpn. J. Appl. Phys.* 42 (2003) 4111–4115.
- [11] D.-S. Kim, Y.-T. Jeong, H.-K. Lyu, H.-J. Park, J.-K. Shin, P. Choi, J.-H. Lee, G. Lim, An FET-type charge sensor for highly sensitive detection of DNA sequence, *Biosens. Bioelectron.* 20 (2004) 69–74.
- [12] D.-S. Kim, H.-J. Park, H.-M. Jung, J.-K. Shin, Y.-T. Jeong, P. Choi, J.-H. Lee, G. Lim, Field-effect transistor-based biomolecular sensor employing a Pt reference electrode for the detection of deoxyribonucleic acid sequence, *Jpn. J. Appl. Phys.* 43 (2004) 3855–3859.
- [13] F. Uslu, S. Ingebrandt, D. Mayer, S. Böcker-Meffert, M. Odenthal, A. Offenhäusser, Label-free fully electronic nucleic acid detection system based on a field-effect transistor device, *Biosens. Bioelectron.* 19 (2004) 1723–1731.
- [14] M.W. Dashiell, A.T. Kalambur, R. Leeson, K.J. Roe, J.F. Rabolt, J. Kolodzey, The electrical effects of DNA as the gate electrode of MOS transistors, in: *Proceeding of the IEEE Lester Eastman Conference, Delaware, 2002*, pp. 259–264.
- [15] H. Berney, J. West, E. Haeefe, J. Alderman, W. Lane, J.K. Collins, A DNA diagnostic biosensor: development, characterisation and performance, *Sens. Actuators B* 68 (2000) 100–108.
- [16] F. Pouthas, C. Gentil, D. Cote, U. Bockelmann, DNA detection on transistor arrays following mutation-specific enzymatic amplification, *Appl. Phys. Lett.* 84 (2004) 1594–1596.
- [17] P. Bergveld, A critical evaluation of direct electrical protein detection methods, *Biosens. Bioelectron.* 6 (1991) 55–72.
- [18] G.F. Blackburn, Chemically sensitive field-effect transistors, in: A.P.F. Turner, I. Karube, G.S. Wilson (Eds.), *Biosensors: Fundamentals and Applications*, Oxford University Press, Oxford, 1987, pp. 481–530.
- [19] M.J. Schöning, A. Poghossian, Recent advances in biologically sensitive field-effect transistors, *Analyst* 127 (2002) 1137–1151.

- [20] G.S. Manning, The molecular theory of polyelectrolyte solution with applications to the properties of polynucleotides, *Q. Rev. Biophys.* II (1978) 179–246.
- [21] G.S. Manning, Counterion condensation on a helical charge lattice, *Macromolecules* 34 (2001) 4650–4655.
- [22] S. Bone, C.A. Small, Dielectric studies of ion fluctuation and chain bending in native DNA, *Biochim. Biophys. Acta* 1260 (1995) 85–93.
- [23] P. Sens, J.-F. Joanny, Counterion release and electrostatic adsorption, *Phys. Rev. Lett.* 84 (2000) 4862–4865.
- [24] L. Bousse, N.F. de Rooij, P. Bergveld, Operation of chemically sensitive field-effect sensors as a function of the insulator-electrolyte interface, *IEEE Trans. Electron Devices* ED-30 (1983) 1263–1270.
- [25] K.A. Melzak, C.S. Sherwood, R.F.B. Turner, C.A. Haynes, Driving forces for DNA adsorption to silica in perchlorate solutions, *J. Colloid Interface Sci.* 181 (1996) 635–644.
- [26] W. Yang, J.E. Butler, J.N. Russell Jr., R.J. Hamers, Interfacial electrical properties of DNA-modified diamond thin films: intrinsic response and hybridization-induced field effects, *Langmuir* 20 (2004) 6778–6787.
- [27] V. Chan, S.E. McKenzie, S. Surrey, P. Fortina, D.J. Graves, Effect of hydrophobicity and electrostatics on adsorption of DNA oligonucleotides at liquid/solid interfaces, *J. Colloid Interface Sci.* 203 (1998) 197–207.
- [28] Z. Lin, T. Strother, W. Cai, X. Cao, L.M. Smith, R.J. Hamers, DNA attachment and hybridization at the silicon (1 00) surface, *Langmuir* 18 (2002) 788–796.
- [29] Y. Belosludtsev, B. Iverson, S. Lemeshko, R. Eggers, R. Wiese, S. Lee, T. Powdrill, M. Hogan, DNA microarrays based on noncovalent oligonucleotide attachment and hybridization in two dimensions, *Anal. Biochem.* 292 (2001) 250–256.
- [30] A.G. Cherstvy, A.A. Kornyshev, S. Leikin, Torsional deformation of double helix in interaction and aggregation of DNA, *J. Phys. Chem. B* 108 (2004) 6508–6518.
- [31] A.G. Cherstvy, A.A. Kornyshev, S. Leikin, Temperature dependent DNA condensation triggered by rearrangement of adsorbed cations, *J. Phys. Chem. B* 106 (2002) 13362–13369.
- [32] A.G. Cherstvy, R.G. Winkler, Complexation of semiflexible chains with oppositely charged cylinder, *J. Chem. Phys.* 120 (2004) 9394–9400.